Perinatal High Fat Diet Exposure Alters Oxytocin and Corticotropin Releasing Factor Inputs onto Vagal Neurocircuits Controlling Gastric Motility

Kaitlin E. Carson, Jared Alvarez[1], Jasmine Mackley[2], Alberto Travagli[3] and Kirsteen N. Browning[*]

Department of Neural and Behavioral Sciences, Pennsylvania State College of Medicine, Hershey, PA

[1]Barrett Honors College, Arizona State University, Tempe, AZ.

[2]Schreyer Honors College, Pennsylvania State University, State College, PA

[3] Neurobiology Research, Newport, NC

*Address for correspondence:

Kirsteen N. Browning, PhD,

Penn State College of Medicine,

500 University Drive, MC H109,

Hershey, PA, 17033;

Email: kbrowning@pennstatehealth.psu.edu

ORCID: 0000-0002-5062-3703

Abstract

Perinatal high fat diet (pHFD) exposure alters the development of vagal neurocircuits that control gastrointestinal (GI) motility and reduce stress resiliency in offspring. Descending oxytocin (OXT; prototypical anti-stress peptide) and corticotropin releasing factor (CRF; prototypical stress peptide) inputs from the paraventricular nucleus (PVN) of the hypothalamus to the dorsal motor nucleus of the vagus (DMV) modulate the GI stress response. How these descending inputs, and their associated changes to GI motility and stress responses, are altered following pHFD exposure are, however, unknown. The present study used *in vivo* recordings of gastric tone and motility and gastric emptying rates, *in vitro* electrophysiological recordings from brainstem slice preparations, and retrograde neuronal tracing experiments to investigate the hypothesis that pHFD alters descending PVN-DMV inputs, dysregulating vagal efferent control of gastric motility in response to stress. Rats exposed to pHFD had slower gastric emptying rates, and did not respond to acute stress with the expected delay in gastric emptying. Neuronal tracing experiments demonstrated that pHFD reduced the number of PVN^{OXT} neurons, but increased PVN^{CRF} neurons, that project to the DMV. Both in vitro electrophysiology recordings of DMV neurons and in vivo recordings of gastric motility and tone demonstrated that, following pHFD, PVN^{CRF}-DMV projections were tonically active, and that pharmacological antagonism of brainstem CRF1 receptors restored the appropriate gastric response to brainstem OXT application. These results suggest that pHFD exposure disrupts descending PVN-DMV inputs, leading to altered basal gastric motility as well as maladaptive gastric stress responses and reduced stress resiliency.

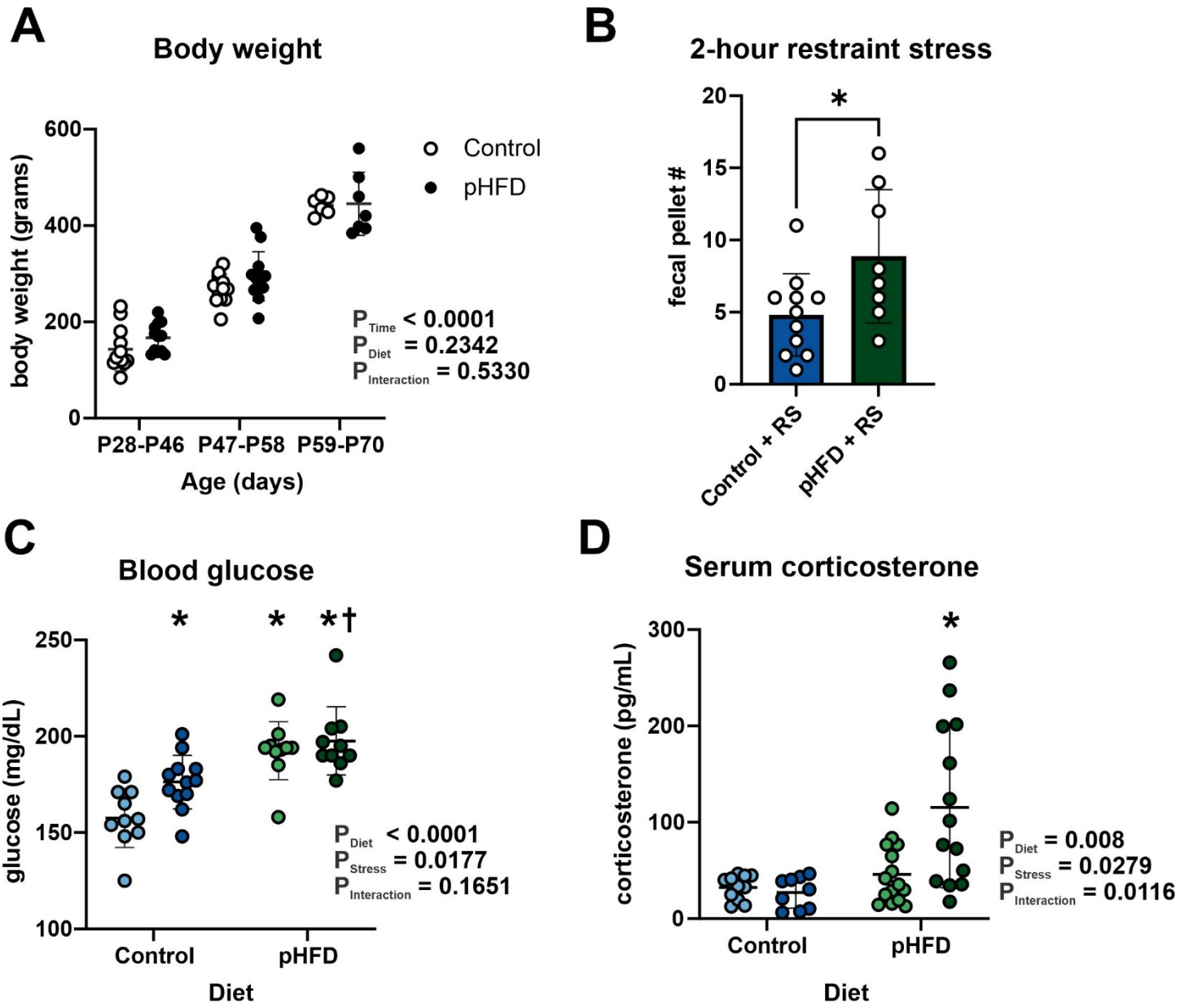
A
Body weight
body weight (grams)
600
400
200
0
Control
pHFD
P28-P46
P47-P58
P59-P70
Age (days)
P Time < 0.0001
P Diet = 0.2342
P Interaction = 0.5330
B
2-hour restraint stress
fecal pellet #
20
15
10
5
0
*
Control + RS
pHFD + RS
C
Blood glucose
glucose (mg/dL)
250
200
150
100
*
*
*†
Control
pHFD
Diet
P Diet < 0.0001
P Stress = 0.0177
P Interaction = 0.1651
D
Serum corticosterone
corticosterone (pg/mL)
300
200
100
0
*
Control
pHFD
Diet
P Diet = 0.008
P Stress = 0.0279
P Interaction = 0.0116

FIGURE ONE: pHFD exposure does not impact body weight, however increases fecal pellet output following stress and elevates blood glucose levels.

A: Graphical summary of body weights (g) in control (N= 6-12) and pHFD (N= 7-12) rats at 3 time points; P28-P46, P47-P58, and P56-P70. Data demonstrate time, but not diet, affect body weight and therefore pHFD rats are not overweight, or obese, compared to age-matched control rats (Mixed-effects model with REML estimation; $p<0.05$ for significant effect). **B:** Graphical summary of fecal pellet output (#) during the 2-hour restraint stress in control (N=11) and pHFD (N=8) rats. pHFD rats are shown to produce significantly more fecal pellets during the acute stressor (* $p<0.05$ using two-way unpaired t-test). **C:** Graphical summary of blood glucose levels (mg/dL) of control (N=10, light blue), control + RS (N=12, dark blue), pHFD (N=10, light green), and pHFD + RS (N=10, dark green) at time of tissue collection. A two-way ANOVA analysis, with diet and stress as variables, reveal that both affect blood glucose levels but that they do not interact ($p<0.05$ denotes a significant effect). *Post-hoc* Bonferroni multiple comparisons test indicate that blood glucose levels are significantly elevated in control + RS and both pHFD groups compared to unstressed controls (* $p<0.05$), demonstrating that stress and exposure to a pHFD elevates blood glucose levels. Additionally, blood glucose levels are elevated in pHFD + RS rats compared to control + RS rats († $p<0.05$) indicating that pHFD exposure exacerbates the stress-induced elevations in blood glucose levels. **D:** Graphical summary of serum corticosterone levels (pg/mL) of control (N=10, light blue), control + RS (N=9, dark blue), pHFD (N=13, light green), and pHFD + RS (N=14, dark green) rats at time of tissue collection. A two-way ANOVA analysis reveals that diet, stress, and their interaction have significant effects on serum corticosterone levels ($p<0.05$ denotes significance). *Post-hoc* Bonferroni multiple comparisons test indicate that while corticosterone levels have returned to unstressed levels in control animals after the 2-hour restraint stress, in pHFD rats levels remain significantly elevated after the stressor (* $p<0.05$ compared to all groups).

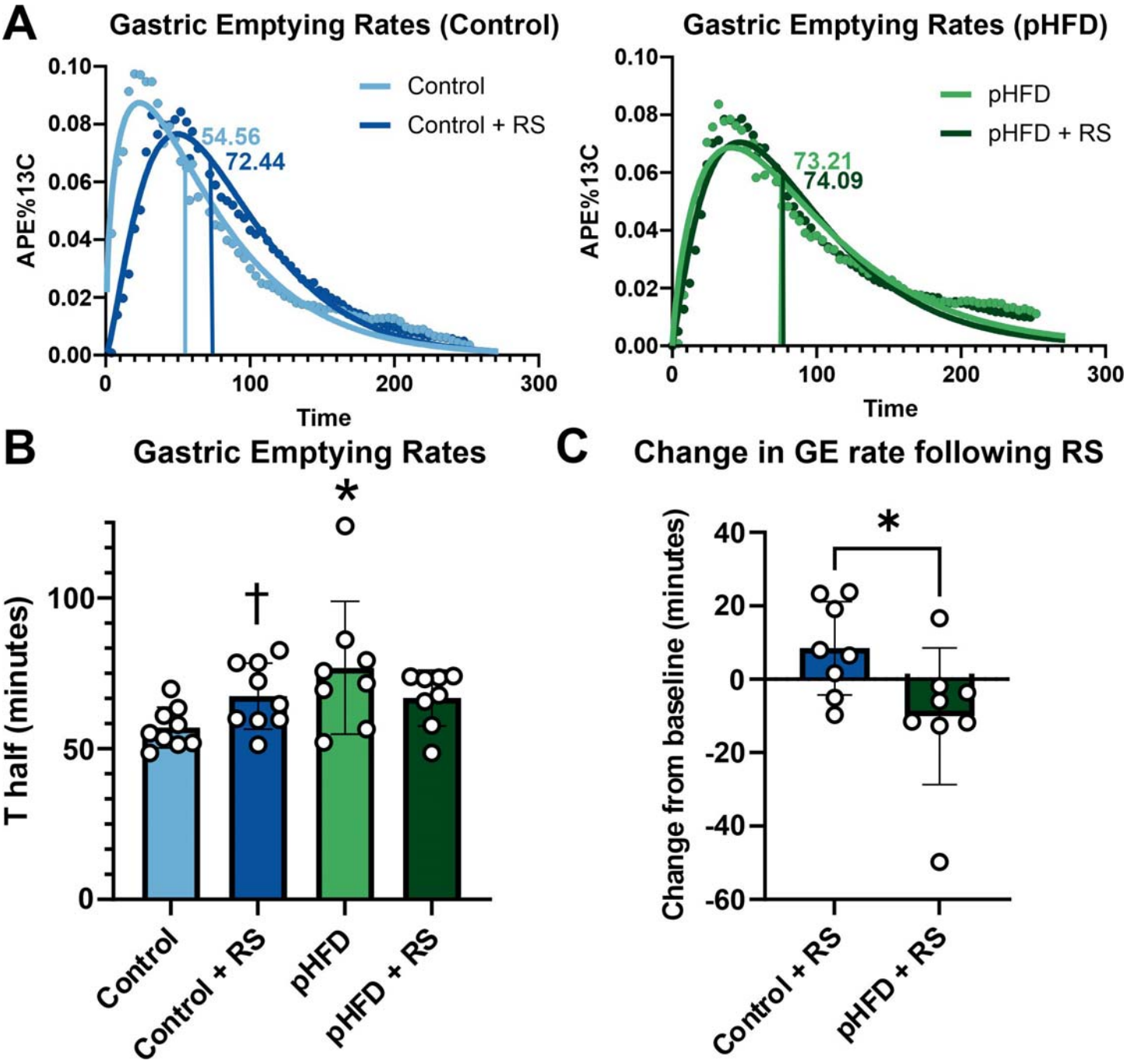
A
Gastric Emptying Rates (Control)
Control
Control + RS
54.56
72.44
APE%13C
Time
Gastric Emptying Rates (pHFD)
pHFD
pHFD + RS
73.21
74.09
APE%13C
Time
B
Gastric Emptying Rates
T half (minutes)
Control
Control + RS
pHFD
pHFD + RS
C
Change in GE rate following RS
Change from baseline (minutes)
Control + RS
pHFD + RS

FIGURE TWO: pHFD rats have slower basal gastric emptying rates and do not mount a gastric stress response.

A: Representative gastric emptying curves of control (light blue), control + RS (dark blue), pHFD (light green), and pHFD + RS (dark green) rats. Vertical lines indicate the $T_{1/2}$ values. The curves illustrate that a 2-hour restraint stress delays gastric emptying rates (seen by an increase in $T_{1/2}$ value) in control rats, however does not affect pHFD rats. **B:** Graphical summary of gastric emptying rates in control rats before and after stress exposure (N=9), as well as pHFD rats before and after stress exposure (N=8). Data indicate that following a 2-hour restraint stress, control rats have significantly delayed gastric emptying rates, whereas pHFD rats do not show a significant delay in their gastric emptying following stress († $p<0.05$ using a two-tailed paired t-test comparing unstressed and stressed $T_{1/2}$ values among diet groups). Additionally, when looking at the unstressed (basal) gastric emptying rates across diet groups, pHFD were found to have significantly slower basal gastric emptying rates (* $p<0.05$ using a two-tailed unpaired t-test compared unstressed control to unstressed pHFD $T_{1/2}$ values). **C:** Graphical summary of the change in gastric emptying rates after stress (stressed-unstressed) in minutes. Data indicate that there is a significant change (in minutes) after a stress between both diet groups, showing that stress affects control and pHFD exposed rats differently (* $p<0.05$ using a two-tailed unpaired t-test comparing the change in $T_{1/2}$ values).

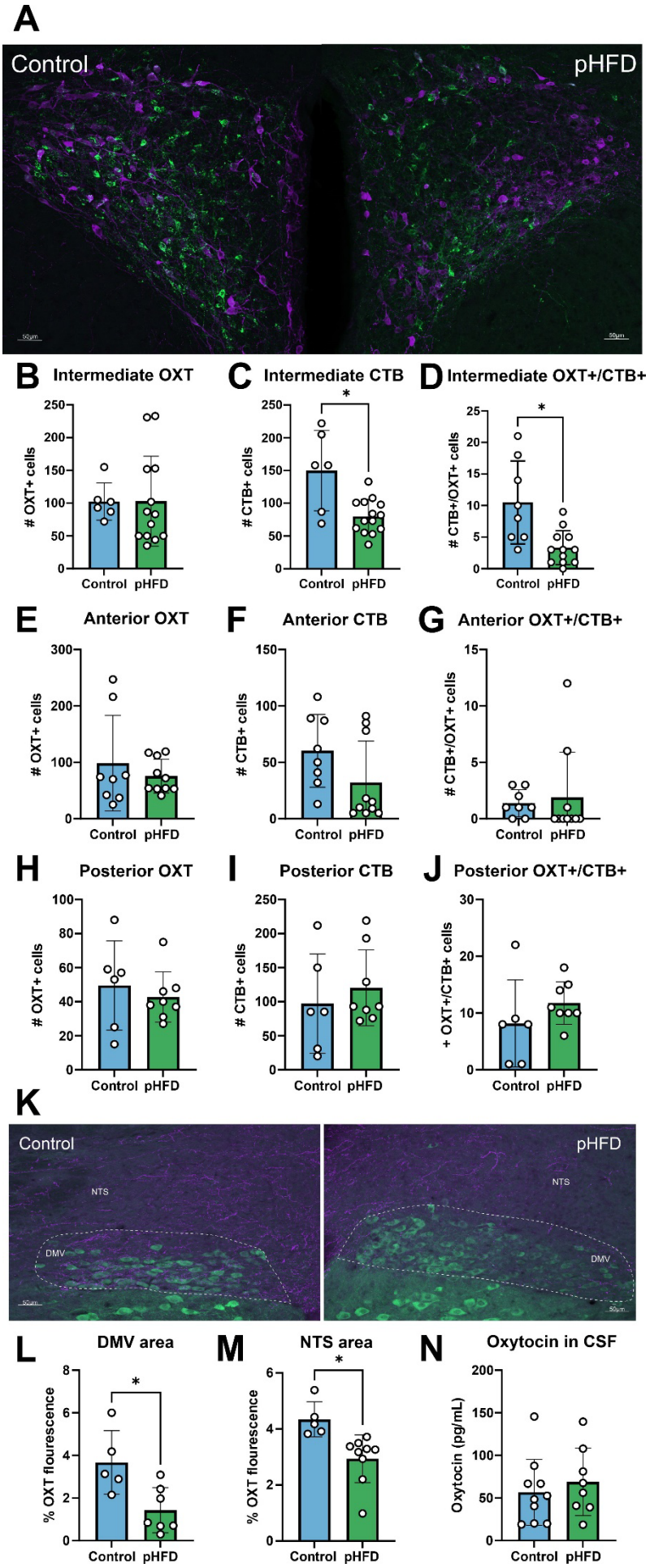
A
Control
pHFD
B Intermediate OXT
OXT+ cells
C Intermediate CTB
CTB+ cells
D Intermediate OXT+/CTB+
CTB+/OXT+ cells
E Anterior OXT
OXT+ cells
F Anterior CTB
CTB+ cells
G Anterior OXT+/CTB+
CTB+/OXT+ cells
H Posterior OXT
OXT+ cells
I Posterior CTB
CTB+ cells
J Posterior OXT+/CTB+
+ OXT+/CTB+ cells
Control
pHFD
K
Control
pHFD
NTS
DMV
L DMV area
% OXT flourescence
M NTS area
% OXT flourescence
N Oxytocin in CSF
Oxytocin (pg/mL)

FIGURE THREE: pHFD exposure decreases DMV-projecting PVN^{OXT} neurons and reduces OXT fiber expression in the DMV and NTS.

A: Representative images of the intermediate PVN with CTB+ neurons in green and OXT+ neurons in magenta from a control (left) and pHFD (right) rat. pHFD (N=4) and control (N=4) rats received a microinjection of the retrograde tracer CTB in the DMV to visualize DMV-projecting neurons in the hypothalamus. Images were taken at 20X magnification and cells were quantified by manual counting, with co-localization identified by a white fluorescent signal on both the left and right side. Representative images illustrate the loss in CTB+ cells in pHFD rats. **B:** Graphical summary of quantification of OXT+ cells in the intermediate PVN, showing no difference between control and pHFD rats. **C:** Graphical summary of quantification of CTB+ neurons in the intermediate PVN, showing there was a significant reduction in DMV-projecting neurons in pHFD rats (* $p<0.05$ using a two-tailed unpaired t-test). **D:** Graphical summary of quantification of neurons with OXT and CTB co-localization, showing there is a significant reduction of DMV-projecting PVN^{OXT} neurons in pHFD rats (* $p <0.05$ using two-tailed unpaired t-test). Quantification of neurons in the anterior PVN found no differences in the number of OXT+ (**E**), CTB + (**F**), and OXT+/CTB+ (**G**) cells between diet groups. Quantification of neurons in the posterior PVN found no differences in the number of OXT+ (**H**), CTB+ (**I**), and OXT+/CTB+ (**J**) cells between diet groups. **K:** Representative images of the brainstem containing the DMV (outlined) and NTS. Cholinergic neurons (green) were visualized to identify the DMV and OXT+ fibers were visualized with magenta. Images were taken at 20X magnification and OXT fibers were quantified using % fluorescence within the selected region (either DMV or NTS) on both the left and right side. Representative images illustrate the loss of oxytocin fibers in pHFD rats. **L:** Graphical summary of % OXT fluorescence in the DMV where pHFD (N=4) rats show a significant reduction compared to controls (N=4) (* $p<0.05$ using a two-tailed unpaired t-test). **M:** Graphical summary of % OXT fluorescence in the NTS where pHFD rats (N=4) show a significant reduction compared to controls (N=4) (* $p<0.05$ using a two-tailed unpaired t-test). **N:** Graphical summary of oxytocin levels within CSF samples taken from pHFD (N=8) and control (N=10) rats. Data indicate there is not a significant difference between the diet groups.

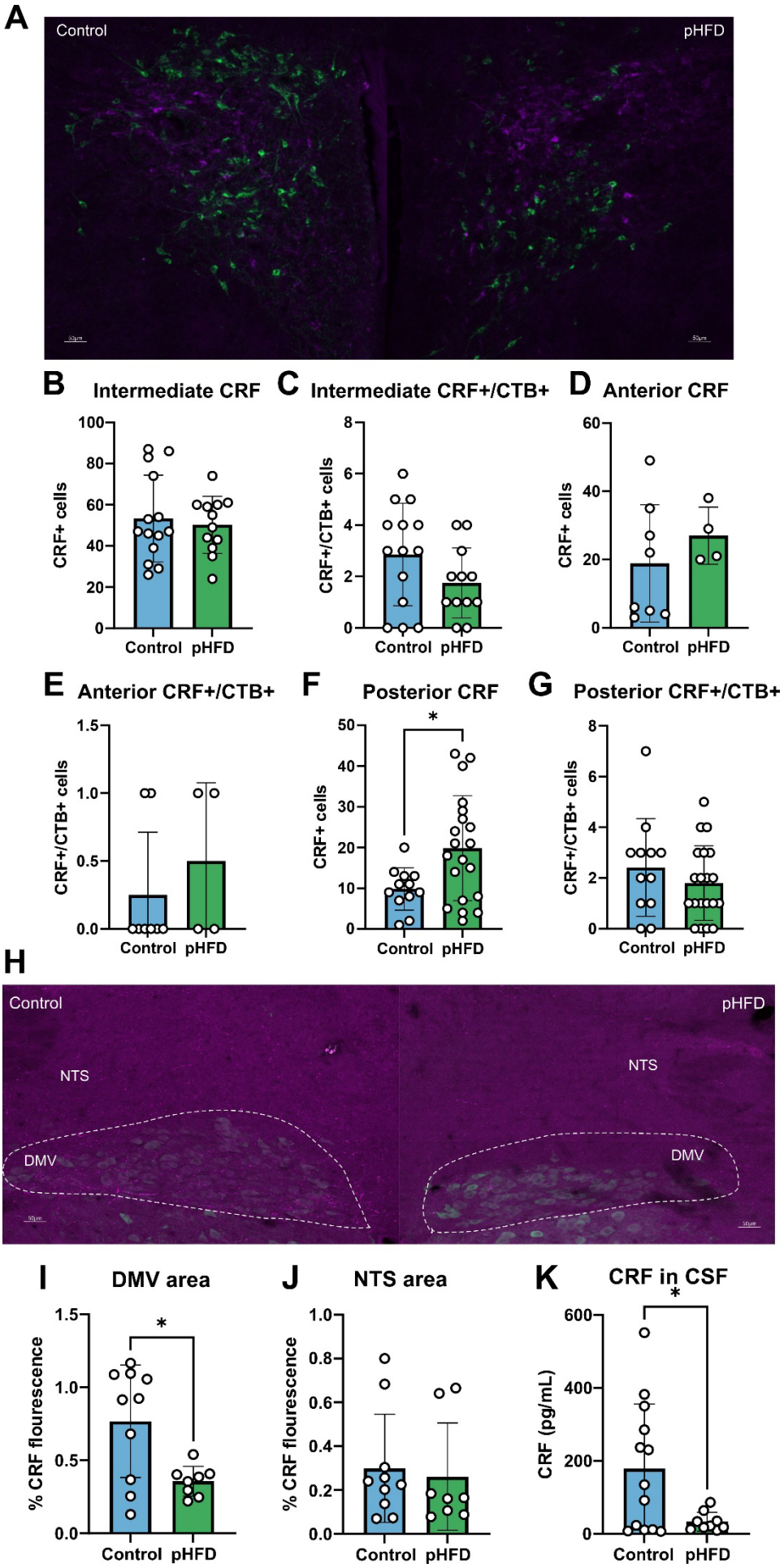
A
Control
pHFD
B
Intermediate CRF
CRF+ cells
Control
pHFD
C
Intermediate CRF+/CTB+
CRF+/CTB+ cells
D
Anterior CRF
E
Anterior CRF+/CTB+
F
Posterior CRF
*
G
Posterior CRF+/CTB+
H
NTS
DMV
I
DMV area
% CRF flourescence
J
NTS area
K
CRF in CSF
CRF (pg/mL)

FIGURE FOUR: pHFD exposure increases PVN^{CRF} neurons, however reduces CRF fibers in the DMV and CRF protein levels in the CSF.

A: Representative images of the intermediate PVN with CTB+ neurons in green and CRF+ neurons in magenta from a control (left) and pHFD (right) rat. pHFD (N=4) and control (N=4) rats received a microinjection of the retrograde tracer CTB in the DMV to visualize DMV-projecting neurons in the hypothalamus. Images were taken at 20X magnification and cells were quantified by manual counting, with co-localization identified by a white fluorescent signal on both the left and right side. Representative images illustrate the loss in CTB+ cells in pHFD rats. Quantification of CRF+ neurons (**B**) and CRF+/CTB+ neurons (**C**) in the intermediate PVN show no significant difference between diet groups. Similarly, quantification of CRF+ neurons (**D**) and CRF+/CTB+ neurons (**E**) in the anterior PVN no significant difference between diet groups. **F:** Graphical summary of the number of CRF neurons in the posterior PVN demonstrating a significant increase in CRF neurons in pHFD rats compared to controls (* $p<0.05$ using a two-tailed unpaired t-test). **G:** Graphical summary of the number of neurons with CRF and CTB co-localization in the anterior PVN, showing no significant difference between pHFD and control rats. **H:** Representative images of the brainstem containing the DMV (outlined) and NTS. Cholinergic neurons (green) were visualized to identify the DMV and CRF+ fibers were visualized with magenta. Images were taken at 20X magnification and CRF fibers were quantified using % fluorescence within the selected region (either DMV or NTS) on both the left and right side. Representative images illustrate the loss of CRF fibers in the DMV of pHFD rats. **I:** Graphical summary of % CRF fluorescence in the DMV where pHFD rats (N=4) show a significant reduction compared to controls (N=4) (* $p<0.05$ using a two-tailed unpaired t-test). **J:** Graphical summary of % CRF fluorescence in the NTS showing there is no difference between pHFD (N=4) and control (N=4) rats. **K:** Graphical summary of CRF levels within CSF samples taken from pHFD (N=9) and control (N=13) rats. Data indicate there is significantly less CRF protein in the CSF of pHFD rats (* $p<0.05$ using a two-tailed unpaired t-test).

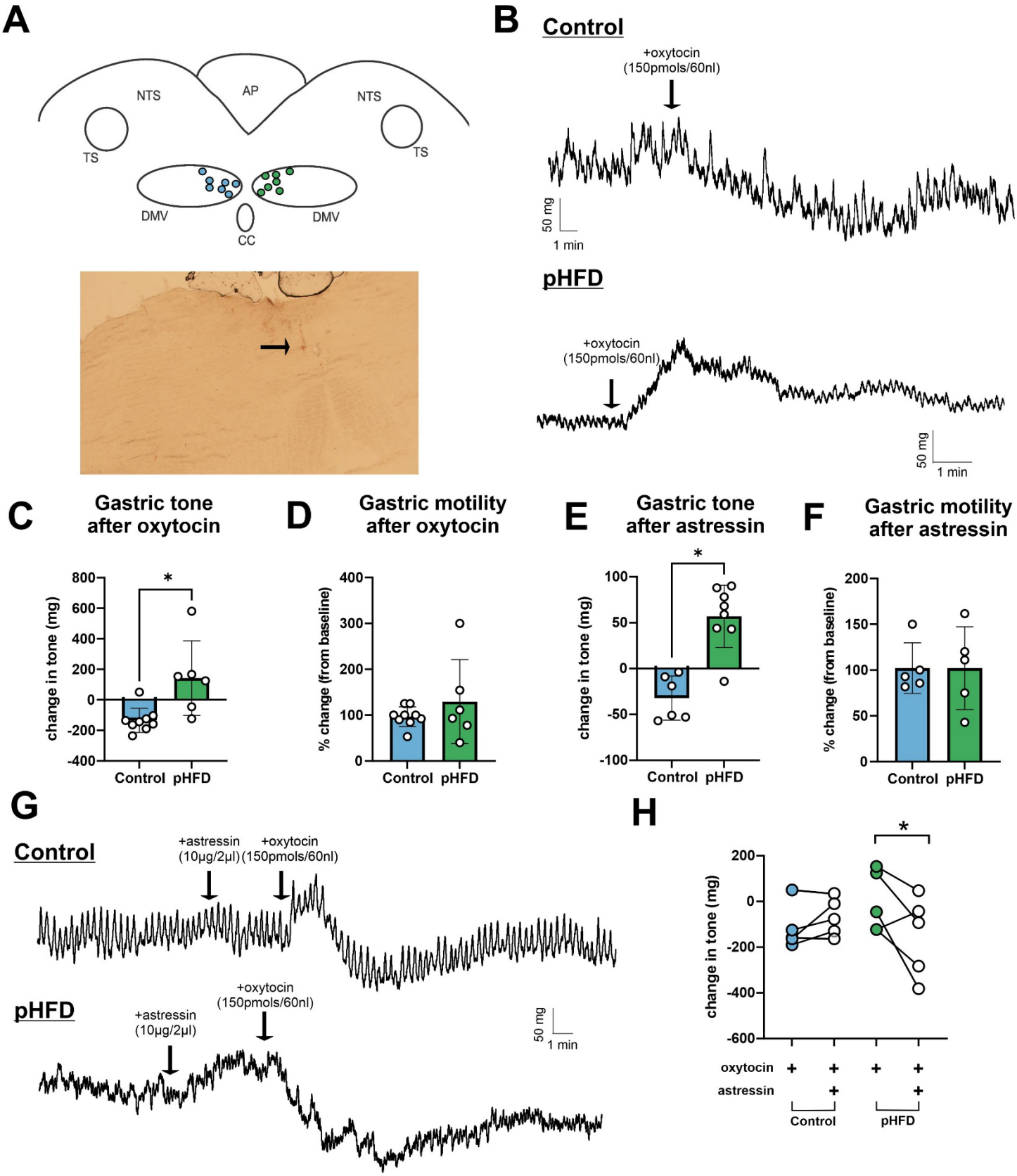
A
NTS
AP
NTS
TS
TS
DMV
DMV
CC
B
Control
+oxytocin
(150pmols/60nl)
50 mg
1 min
pHFD
+oxytocin
(150pmols/60nl)
50 mg
1 min
C
Gastric tone
after oxytocin
change in tone (mg)
800
600
400
200
0
-200
-400
*
Control
pHFD
D
Gastric motility
after oxytocin
% change (from baseline)
400
300
200
100
0
Control
pHFD
E
Gastric tone
after astressin
change in tone (mg)
100
50
0
-50
-100
*
Control
pHFD
F
Gastric motility
after astressin
% change (from baseline)
200
150
100
50
0
Control
pHFD
G
Control
+astressin
(10µg/2µl)
+oxytocin
(150pmols/60nl)
pHFD
+astressin
(10µg/2µl)
+oxytocin
(150pmols/60nl)
50 mg
1 min
H
change in tone (mg)
200
0
-200
-400
-600
*
oxytocin + + + +
astressin + +
Control
pHFD

FIGURE FIVE: pHFD rats have dysregulated gastric motility that resembles a stressed phenotype which is rescued by a CRF receptor antagonist.

A: Schematic (top) showing the microinjection sites of oxytocin in control (N=7, light blue circles) and pHFD (N=7, light green circles) animals for *in vivo* recordings of gastric corpus motility. All injections were made on the left side of the DMV, but are separated out on the schematic for clarity. A representative image of a coronal section of the brainstem (bottom) is shown with an arrow pointing to the track of the microinjection pipette that is used to verify the injection site. **B:** Representative traces of *in vivo* recordings of corpus gastric tone and motility of a control (top) and pHFD (rat) that received a microinjection of oxytocin into the DMV. The traces demonstrate that in a control animal, oxytocin injection leads to a decrease in tone, whereas in a pHFD animal there is an increase in tone. Also demonstrated is the larger basal motility (evidenced by larger peaks) in the control animal recording. **C:** Graphical summary of the change in tone (in mg) after microinjection of oxytocin into the DMV in control (N=9) and pHFD (N=6) groups. A two-tailed unpaired t-test shows that the change in tone is significantly different in pHFD rats compared to controls (* $p<0.05$). Specifically, pHFD rats show an increase in tone in response to oxytocin microinjection. **D:** Graphical summary of the change in motility (as a % of the baseline motility) in control (N=9) and pHFD (N=6) rats. The data indicate there is no significant difference in the motility response to oxytocin microinjection between the diet groups. **E:** Graphical summary of the change in tone (in mg) after astressin application on the 4th ventricle in control (N=6) and pHFD (N=8) rats. The data show that there is a significant difference between the response to astressin in control and pHFD animals (* $p<0.05$ using a two-tailed unpaired t-test). **F:** Graphical summary of the change in motility in control (N=5) and pHFD (N=5) after 4th ventricular application of astressin. The data demonstrate that there is not a significant difference in the motility response to astressin application between diet groups. **G:** Representative traces of *in vivo* recordings of corpus gastric tone and motility of a control (top) and pHFD (rat) who received 4th ventricular application of astressin followed by a microinjection of oxytocin into the DMV. In the control trace, astressin application did not shift tone, and oxytocin application led to a decrease in tone, suggesting there is no tonic CRF release and therefore did not impact the gastric response to oxytocin. However, in the pHFD trace, astressin application led to an increase in tone, followed by which oxytocin microinjection led to a decrease in tone. This would suggest that in pHFD animals there is a tonic CRF input onto central vagal neurocircuits, and by pharmacologically blocking them the gastric response to oxytocin was normalized (resembles control animals). **H:** Graphical summary of the change in tone after initial oxytocin microinjection (filled circles), followed by a second oxytocin microinjection in the presence of 4th ventricular supplication of astressin (open circles) in control (N=) and pHFD (N=) rats. The data show that in control animals, astressin application has no effect on oxytocin's change in gastric tone. However, in pHFD rats, astressin application leads oxytocin microinjection to cause a decrease in tone (* $p<0.05$ using a two-tailed paired t-test comparing oxytocin's change in tone before and after astressin application). These data suggest that the oxytocin-induced changes in gastric tone can be normalized by blocking CRF receptors.

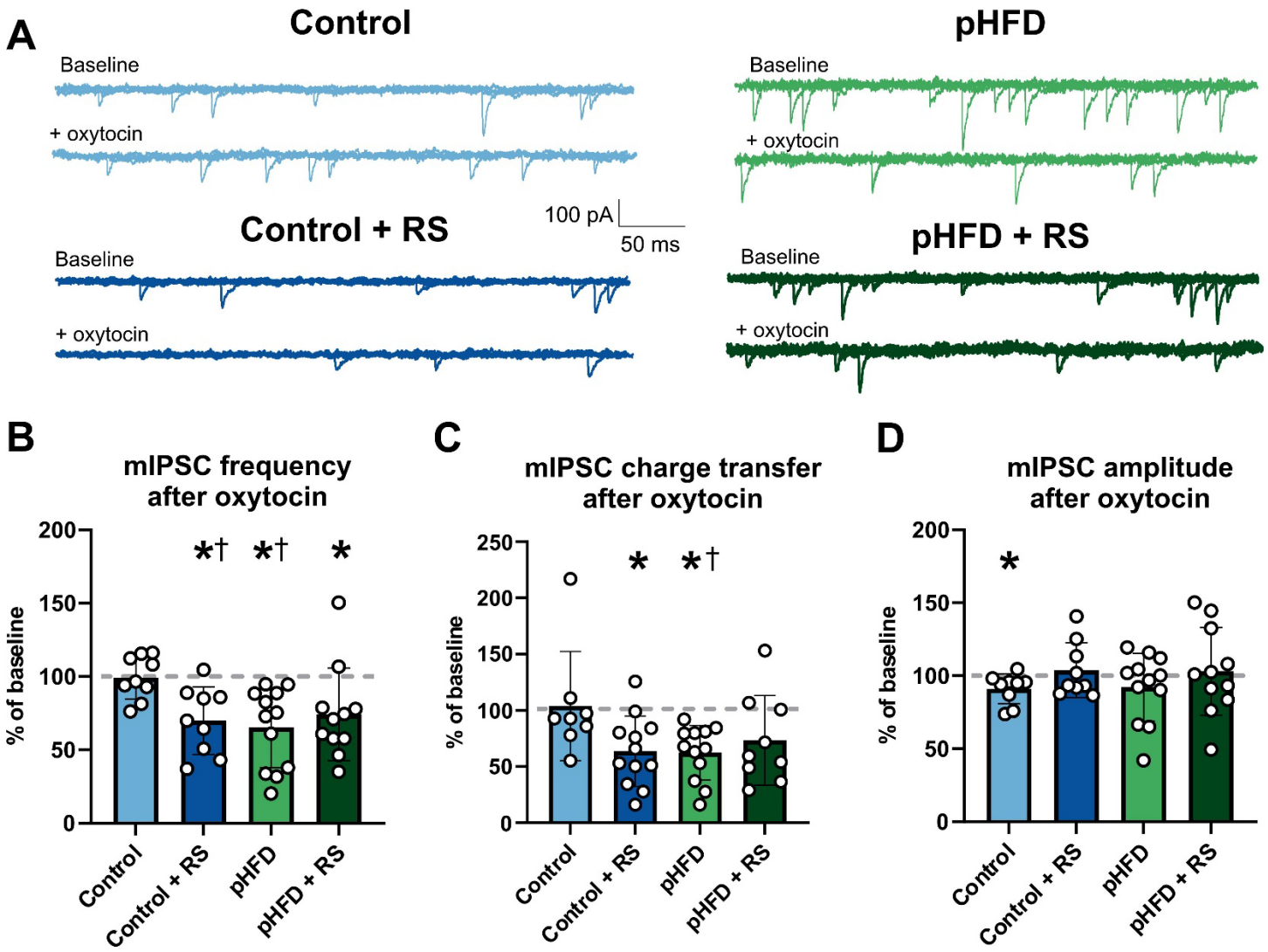
A
Control
Baseline
+ oxytocin
pHFD
Baseline
+ oxytocin
100 pA
50 ms
Control + RS
Baseline
+ oxytocin
pHFD + RS
Baseline
+ oxytocin
B
mIPSC frequency after oxytocin
% of baseline
200
150
100
50
0
*†
*†
*
Control
Control + RS
pHFD
pHFD + RS
C
mIPSC charge transfer after oxytocin
% of baseline
250
200
150
100
50
0
*
*†
Control
Control + RS
pHFD
pHFD + RS
D
mIPSC amplitude after oxytocin
% of baseline
200
150
100
50
0
*
Control
Control + RS
pHFD
pHFD + RS

FIGURE SIX: pHFD exposure uncovers OXT-mediated inhibition of GABAergic synaptic currents.

A: Representative traces of miniature inhibitory post synaptic currents (mIPSCs) recorded from control (light blue), pHFD (light green), control + RS (dark blue), and pHFD + RS (dark green) DMV neurons before (top trace) and after (bottom trace) application of oxytocin. Baseline conditions were recorded in the presence of TTX and kynurenic acid to isolate mIPSCs. Recordings illustrate that in control neurons, oxytocin application does not change the frequency of mIPSCs. However, in the other three groups, oxytocin application leads to a decrease in mIPSC frequency. **B:** Graphical summary of the change in frequency of mIPSCs after oxytocin application (as a % of the baseline) in control (N=9), control + RS (N=9), pHFD (N=12), and pHFD + RS (N=11) cells. The data indicate that oxytocin does not alter mIPSC frequency on control cells, however after stress or exposure to a pHFD, oxytocin induces a significant decrease in mIPSC frequency (* $p<0.05$ using a two-tailed one sample t-test against a theoretical mean of 100 (representing no change from baseline)). Furthermore, stress or pHFD exposure significantly changes the oxytocin-mediated change in mIPSC frequency from control neurons († $p<0.05$ using a two-tailed unpaired t-test compared to the control group). These data indicate that stress and pHFD exposure uncover a presynaptic effect of oxytocin on inhibitory currents on DMV neurons. **C:** Graphical summary of the change in charge transfer of mIPSCs after oxytocin application (as a % of the baseline). Charge transfer was calculated as mIPSC frequency/mIPSC area, then compared before (baseline) and after oxytocin application. The results indicate that, like changes in mIPSC frequency, stress and pHFD exposure induce an oxytocin-mediated decrease in mIPSC charge transfer (* $p<0.05$ using a two-tailed one sample t-test against a theoretical mean of 100 (representing no change from baseline)). Additionally, a two-tailed unpaired t-test show that oxytocin revealed a significantly different effect on charge transfer in pHFD cells compared to controls († $p<0.05$). **D:** Graphical summary of the change in mIPSC amplitude after oxytocin application (as a % of baseline). The results indicate that oxytocin application decreases amplitude in only control DMV neurons (* $p<0.05$ using a two-tailed one sample t-test against a theoretical mean of 100 (representing no change from baseline)), and that there were no significant differences amongst diet or stress groups. These results indicate that oxytocin decreases mIPSC amplitude through a postsynaptic mechanism in control neurons, however the mean change (91.13%) does not reach the physiological significance of 75% or lower.

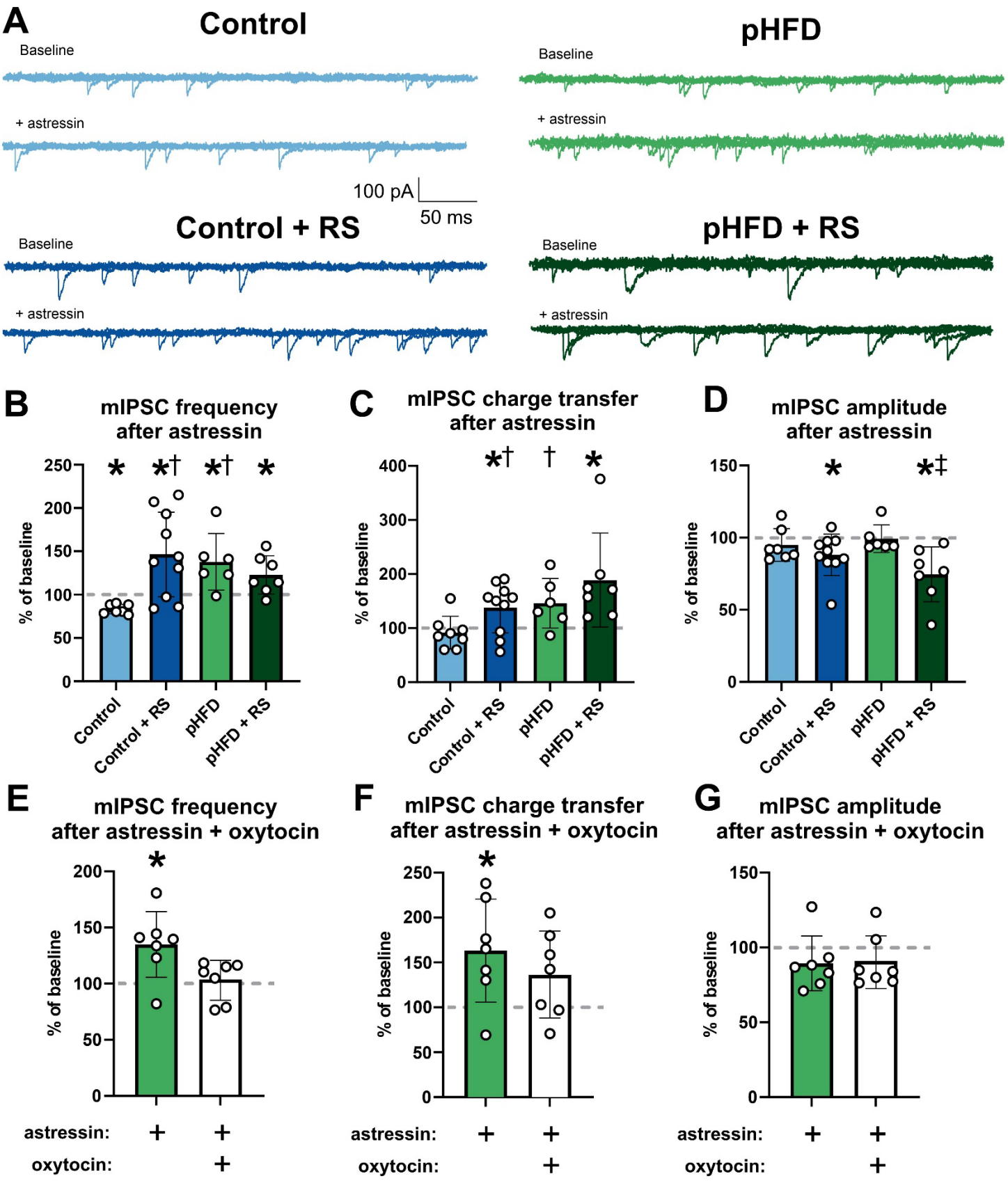
A
Control
Baseline
+ astressin
pHFD
Baseline
+ astressin
100 pA
50 ms
Control + RS
Baseline
+ astressin
pHFD + RS
Baseline
+ astressin
B
mIPSC frequency after astressin
% of baseline
Control
Control + RS
pHFD
pHFD + RS
C
mIPSC charge transfer after astressin
% of baseline
D
mIPSC amplitude after astressin
% of baseline
E
mIPSC frequency after astressin + oxytocin
% of baseline
astressin:
oxytocin:
F
mIPSC charge transfer after astressin + oxytocin
% of baseline
astressin:
oxytocin:
G
mIPSC amplitude after astressin + oxytocin
% of baseline
astressin:
oxytocin:

FIGURE SEVEN: pHFD exposure leads to tonic CRF input onto DMV neurons, leading to a stressed phenotype.

A: Representative traces of miniature inhibitory post synaptic currents (mIPSCs) recorded from control (light blue), pHFD (light green), control + RS (dark blue), and pHFD + RS (dark green) DMV neurons before (top trace) and after (bottom trace) application of astressin. Baseline conditions were recorded in the presence of TTX and kynurenic acid to isolate mIPSCs. Recordings illustrate that in the stress and pHFD groups, astressin application leads to an increase in mIPSC frequency, indicating that there is CRF being released onto these neurons. **B:** Graphical summary of the change in frequency of mIPSCs after astressin application (as a % of the baseline) in control (N=7), control + RS (N=10), pHFD (N=6), and pHFD + RS (N=7) cells. The data indicate that astressin significantly increases mIPSC frequency in control + RS, pHFD, and pHFD + RS cells. Interestingly, the data also show that astressin application leads to a significant reduction in mIPSC frequency in control cells, however the change as a % of baseline (83.3%) does not fulfill a physiologically significant change in frequency (75% or lower) (* $p<0.05$ using a two-tailed one sample t-test against a theoretical mean of 100 (representing no change from baseline)). Furthermore, the change in mIPSC frequency in stress and pHFD exposed neurons was significantly different than control neurons († $p<0.05$ using a two-tailed unpaired t-test compared to the control group). These results indicate that there is tonic release of CRF onto DMV neurons that is acting presynaptically to modulate mIPSCs. **C:** Graphical summary of the change in charge transfer of mIPSCs after astressin application (as a % of the baseline). Charge transfer was calculated as mIPSC frequency/mIPSC area, then compared before (baseline) and after astressin application. These results indicate that stress in both diet groups leads to a significant increase in mIPSC charge transfer in response to astressin application (* $p<0.05$ using a two-tailed one sample t-test against a theoretical mean of 100 (representing no change from baseline)). Similarly to its effects on mIPSC frequency, astressin has significantly different effects on charge transfer in the control + RS and pHFD groups compared to controls († $p<0.05$ using a two-tailed unpaired t-test). **D:** Graphical summary of the change in amplitude after astressin application (as a % of baseline). The data show that astressin significantly reduces mIPSC amplitude in control + RS neurons, however the mean change (88.04% of baseline) is not a physiologically significant change. However, astressin does significantly decrease mIPSC amplitude in pHFD + RS neurons (* $p<0.05$ using a two-tailed one sample t-test against a theoretical mean of 100 (representing no change from baseline)). This change in amplitude was also found to be significantly different from pHFD neurons (‡ $p<0.05$ using a two-tailed unpaired t-test compared to the pHFD group). These results would suggest that CRF is also acting postsynaptically in pHFD + RS neurons to modulate mIPSCs. **E:** Graphical summary of experiments performed to determine if blocking the tonic CRF input onto DMV neurons (via astressin application) would eliminate the oxytocin-induced reductions in mIPSCs frequency in pHFD neurons. Represented is the change in mIPSC frequency after astressin application (light green bar) and the change in mIPSC frequency after oxytocin application in the presence of astressin (white bar) as a % of their respective baselines. Same as previous experiments showed, astressin application led to an increase in mIPSC frequency (* $p<0.05$ using a two-tailed

one sample t-test against a theoretical mean of 100 (representing no change from baseline)). However, when the tonic CRF input is blocked, oxytocin no longer induces a significant decrease in mIPSC frequency. These results would suggest that pHFD neurons are already under stress (via tonic CRF release) and that blocking it normalizes their response to oxytocin, resembling control neurons. **F:** Graphical summary of the same experiments mentioned in (**E**) but instead looking at changes to charge transfer. Similarly, astressin application led to a significant increase in charge transfer of mIPSCs in pHFD neurons ((* $p<0.05$ using a two-tailed one sample t-test against a theoretical mean of 100 (representing no change from baseline)) and oxytocin application in the presence of astressin no longer had an effect. **G:** Graphical summary of the same experiments mentioned in (**E**,**F**) but looking at changes to mIPSC amplitude. As shown previously, astressin application, and oxytocin application in the presence of astressin, did not significantly affect mIPSC amplitude in pHFD neurons